A Non-ZUPT Gait Reconstruction Method for Ankle Sensors

Xiaoxu Wu[1] ,Yan Wang[2], Greg Pottie[3]

Abstract— **Monitoring lower body motion, especially gait pattern, using low cost Inertial Measurement Units on a daily basis is becoming critically important for the diagnosis and rehabilitation of neurological diseases. The current state of the art algorithm is to double integrate motion acceleration and compensate cumulative errors by resetting velocity signals to zero at the stance-phase of each stride. However, this method is only applicable for foot-mounted sensors. For the medically more preferable ankle-mounted position, the assumption of this zero-velocity-update (ZUPT) method does not hold. In this paper, a new non-ZUPT method is proposed. We estimated the true velocity during stance-phase, and reset velocity to the estimated value instead of zero. 10 subjects were recruited for 40-meter-level flat floor walking. The stride length estimation error was reduced to 3.58% from 13.22% on average comparing to the conventional ZUPT method on an ankle-mounted sensor. Validity of this method is further supported by stairs walking of 4 more subjects.**

I. INTRODUCTION

Wireless inertial sensors including accelerometers, gyroscopes and magnetometers allow clinicians and researchers to monitor the quantity and the quality of human activities on a daily basis. With these advances, the urgent need for inexpensive and continuous human motion monitoring system for diagnosis and treatment of neurological conditions can be fulfilled [1][2]. Among different types of human motion analysis, gait analysis, investigating the walking pattern, has been widely used for disease diagnosis and rehabilitation guidance due to its periodicity and frequentness in daily life.

One approach for tracking lower body motion is to use a double pendulum model [3]. But this model needs two sensors on each side (one on the thigh and one on the ankle) for accurate estimation. Moreover, the requirement of correct orientation and placement of the sensors limits its practical application.

The other approach is double integration of the motion acceleration. A zero-velocity-update (ZUPT) method is applied to compensate the cumulative error [4][5][6]. The ZUPT method needs only one sensor and is extensively employed because of its robustness and easy implementation. This ZUPT method assumes that there exists a stable zero-velocity interval within each stride and this critical assumption only holds when the sensor is mounted on the foot. However, in most medical applications, clinicians prefer ankle-mounted positions for lower body motion tracking[7][8][1]. This is because, not all patients wear shoes with laces everyday. It happens fairly often that they don't even wear shoes when it is important to capture activity. In contrast, ankle-mounted sensors allow clinicians to deploy the sensors without considering these constraints. Hence, a new velocity update method for ankle-mounted sensors is needed.

In this paper, a novel non-ZUPT method is proposed. In this non-ZUPT method, the velocity signals are reset to estimated values instead of zeros at the stance-phase of each stride. This stance-phase velocity estimation was calculated using gyroscope measurements and sensor position information. A training process with short walking was deployed to avoid the manual measurement of sensor position each time the sensor is mounted.

The rest of this paper is structured as follows. After a quick review of the widely used ZUPT method for foot-mounted sensor trajectory estimation, detailed discussion of the novel non-ZUPT method will be described in section II. In section III, experimental design and results are reported. In section IV, conclusions and suggestions for future work are presented.

II. METHOD

A. Experimental Instrumentation

Invensense Motion SDK sensors produce 3D accelerometer measurements (${}^s\mathbf{a}_t$), 3D gyroscope measurements (${}^s\boldsymbol{\omega}_t$), and filtered orientation information in quaternion representation (${}^i\mathbf{q}_t$) with 200Hz sampling rate. The right subscript t represents a sample at time t; the left superscript s represents the measurement in the sensor frame; the left superscript i of the quaternion represents the orientation of the sensor with respect to the initial frame when the sensor was powered on. Data were transmitted through the on-board Bluetooth to a local PC.

Two sensors were mounted on the left ankle and the left foot (Figure 1) of the subject. For the ankle-mounted sensor, performance of the traditional ZUPT and newly-proposed non-ZUPT methods will be compared. In addition, a performance reference is provided by a foot-mounted sensor using ZUPT method.

Fig. 1: Experimental Setup

[1]Xiaoxu Wu and [2]Yan Wang are with the Department of Electrical Engineering, University of California, Los Angeles, xiaoxuwu at ucla.edu, phylliswany at ucla.edu

[3]Greg Pottie is the faculty of the Department of Electrical Engineering, University of California, Los Angeles, pottie at ee.ucla.edu

978-1-4244-7929-0/14/$26.00 ©2014 IEEE

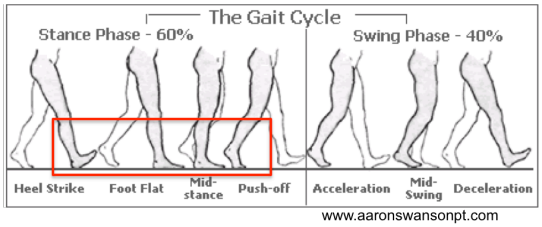

Fig. 2: Gait Segmentation

B. Data Preprocessing

All data collected are preprocessed by the method described in this section. Before the motion starts, a short stable period was required. The sensor frame during this period was considered to be the global reference frame. The average of the accelerometer measurements and quaternions in this period are denoted as ${}^{g}\mathbf{a}_0$ and ${}^{g}\mathbf{q}_0$. The quaternions at any time t can be projected onto the global reference frame with Equation 1.

$$ {}^{g}\mathbf{q}_t = ({}^{g}\mathbf{q}_0)^{-1} \times ({}^{i}\mathbf{q}_t) \tag{1} $$

Using quaternions in the global reference frame, the accelerometer data can be projected onto the global frame with Equation 2, where $\overline{{}^{g}\mathbf{q}_t}$ is the quaternion conjugate of ${}^{g}\mathbf{q}_t$.

$$ \begin{bmatrix} 0 \\ {}^{g}\mathbf{a}_t \end{bmatrix}^T = {}^{g}\mathbf{q}_t \times \begin{bmatrix} 0 \\ {}^{s}\mathbf{a}_t \end{bmatrix}^T \times \overline{{}^{g}\mathbf{q}_t} \tag{2} $$

Since ${}^{g}\mathbf{a}_0$ is a good estimate of gravity in the global frame ${}^{g}\mathbf{G}$, pure motion acceleration in the global frame ${}^{g}\mathbf{a}_t^{Motion}$ can be calculated by subtracting ${}^{g}\mathbf{a}_0$ from ${}^{g}\mathbf{a}_t$ (Equation 3).

$$ \begin{aligned} {}^{g}\mathbf{a}_t^{Motion} &= {}^{g}\mathbf{a}_t - {}^{g}\mathbf{G} \\ &= {}^{g}\mathbf{a}_t - {}^{g}\mathbf{a}_0 \end{aligned} \tag{3} $$

This preprocessing procedure gives motion acceleration ${}^{g}\mathbf{a}_t^{Motion}$ and sensor orientation with respect to the global frame in quaternion ${}^{g}\mathbf{q}_t$.

C. Foot-sensor Gait Reconstruction Using ZUPT

1) stance phase detection: Figure 2 shows the complete gait cycle of a healthy adult. At the middle of each stance-phase, the foot is stable and flat on the ground. These time stamps should be detected before velocity update can be implemented.

A detection method similar to the Acceleration Magnitude Detector in [6] is applied. The average of the motion acceleration energy $\|{}^{g}\mathbf{a}_t^{Motion}\|^2$ in a sliding window (length 0.1s) is evaluated. By selecting the proper threshold ($0.025 m^2/s^4$) , windows of stance phase are detected. The mid-points of these stance-phase windows are denoted as ST_i, where index i means the stance-phase of the i^{th} stride in the whole walking process.

2) velocity update and trajectory estimation: Raw velocity signal (${}^{g}\mathbf{v}_t^{raw}$) calculated by integrating ${}^{g}\mathbf{a}_t^{Motion}$ (Equation 4) has cumulative error because of the noise in the accelerometer. This cumulative error is corrected by resetting ${}^{g}\mathbf{v}_t^{raw}$ to zero at ST_i. Then, a reliable trajectory can be calculated by integrating this corrected velocity (${}^{g}\mathbf{v}_t^{cor}$).

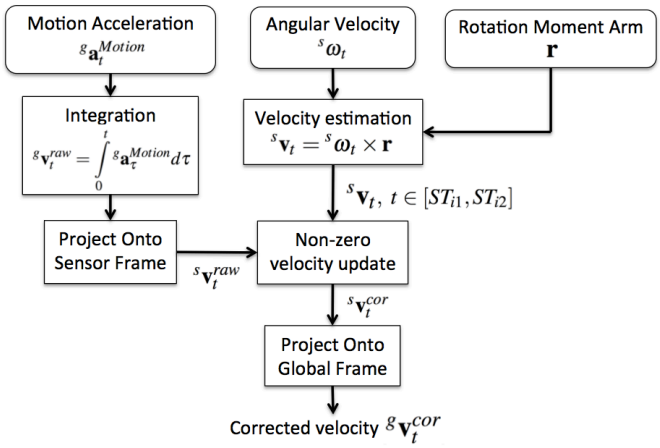

Fig. 3: System Block Diagram For Trajectory Reconstruction

$$ {}^{g}\mathbf{v}_t^{raw} = \int_0^t {}^{g}\mathbf{a}_\tau^{Motion} d\tau \tag{4} $$

D. Ankle-sensor Gait Reconstruction Using Non-ZUPT

For ankle-mounted sensors, the velocity at the middle of the stance phase in each stride is not zero. This velocity can be estimated, and a similar non-ZUPT can be applied.

1) stance phase detection: The average of the motion acceleration energy $\|{}^{g}\omega_t^{Motion}\|^2$ in a sliding window (length 0.1s) is evaluated. By selecting the proper threshold ($2\ rad^2/s^2$) , coarse windows of stance phase are detected. Within each of these coarse windows, a finer window of length 0.05s with the smallest gyroscope energy variance is selected. The starting and ending of this finer window are denoted as ST_{i1} and ST_{i2}, and the center of these fine windows are denoted as ST_i (i = 1...n, n is the total number of strides).

2) velocity update and trajectory estimation: During the stance-phase of each gait cycle, the calf is rotating around the heel (Figure 2). Hence, for an ankle-mounted sensor, the angular velocity ${}^{s}\omega_t$ from gyroscope signals, velocity ${}^{s}\mathbf{v}_t$ and the rotation moment arm $\mathbf{r}$ (determined by the sensor position) are related by Equation 5. The velocity is solved in the sensor frame. This is because, for rotation motion, velocity in the global frame is constantly changing in direction while velocity in the sensor frame is relatively constant.

$$ {}^{s}\mathbf{v}_t = {}^{s}\omega_t \times \mathbf{r},\ , t \in [ST_{i1}, ST_{i2}] \tag{5} $$

Figure 3 shows the system block diagram for the trajectory reconstruction. We start with integrating the pure motion acceleration ${}^{g}\mathbf{a}_t^{Motion}$ and calculating the raw velocity signal ${}^{g}\mathbf{v}_t^{raw}$ (Equation 4). The velocity is then projected into the sensor frame using quaternion information (Equation 6).

$$ \begin{bmatrix} 0 \\ {}^{s}\mathbf{v}_t^{raw} \end{bmatrix}^T = \overline{{}^{g}\mathbf{q}_t} \times \begin{bmatrix} 0 \\ {}^{g}\mathbf{v}_t^{raw} \end{bmatrix}^T \times {}^{g}\mathbf{q}_t \tag{6} $$

The raw velocity signals ${}^{s}\mathbf{v}_t^{raw}$ are reset to ${}^{s}\mathbf{v}_{ST_i}$ at the resetting point ST_i in each stride. This corrected velocity

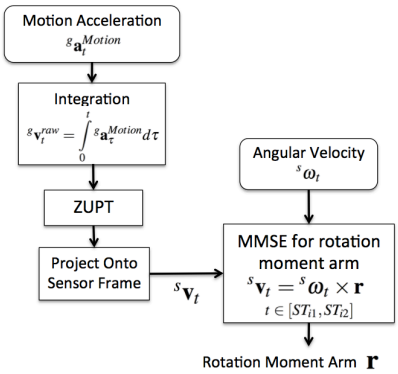

Fig. 4: System Block Diagram For Sensor Position Estimation

${}^{s}\mathbf{v}_t^{cor}$ will be projected back into the global frame (Equation 7). Further integration of ${}^{g}\mathbf{v}_t^{cor}$ will give us the trajectory estimation.

$$\begin{bmatrix} 0 \\ {}^{g}\mathbf{v}_t^{cor} \end{bmatrix}^T = {}^{g}\mathbf{q}_t \times \begin{bmatrix} 0 \\ {}^{s}\mathbf{v}_t^{cor} \end{bmatrix}^T \times \overline{{}^{g}\mathbf{q}_t} \tag{7}$$

3) sensor placement estimation: This non-ZUPT algorithm works only if we know the rotation moment arm $\mathbf{r}$ in Equation 5. A detailed method of estimating $\mathbf{r}$ in a training process will be described below.

In a training process, the subject was asked to do a 3-meter-level short walking on a flat floor. The raw data was preprocessed with the same method described in section II-B. The system block diagram for sensor position estimation is shown in Figure 4.

Similarly, motion acceleration ${}^{g}\mathbf{a}_t^{Motion}$ was first integrated to calculate velocity ${}^{g}\mathbf{v}_t^{raw}$ (Equation 4). Then, ${}^{g}\mathbf{v}_t^{raw}$ was projected onto sensor frame ${}^{s}\mathbf{v}_t^{raw}$ with Equation 6. Because we keep the training process short (3-meter-level walking), resetting the velocity to zero at the starting and ending will correct the cumulative error, and ${}^{g}\mathbf{v}_t^{cor}$ was calculated. The stance-phase window was detected with the method described in section II-D-(1). Finally, the rotation moment arm can be estimated by MMSE using the sampling points over stance-phase windows in Equation 8.

$$\mathbf{r} = \arg\min_{\mathbf{r}} \sum_t \| {}^{s}\mathbf{v}_t^{cor} - {}^{s}\boldsymbol{\omega}_t \times \mathbf{r} \|, \; t \in [ST_{i1}, ST_{i2}] \tag{8}$$

Since the cross product between two three-element column vectors can always be reformulated as product of a matrix and a vector, Equation 8 can be easily solved in normal equation form.

III. EXPERIMENTS AND RESULTS

A. Experimental Procedure

10 subjects were recruited for applying the non-ZUPT algorithm to flat-floor walking. First, in the training process, the subject was asked to perform a 3-meter-level walking (the walking length does not need to be exact). Sensor position information was estimated with the method described in section II-D-(3). Second, in the testing process, the subject performs two sets of 40-meter-level walking on the ruled floor.

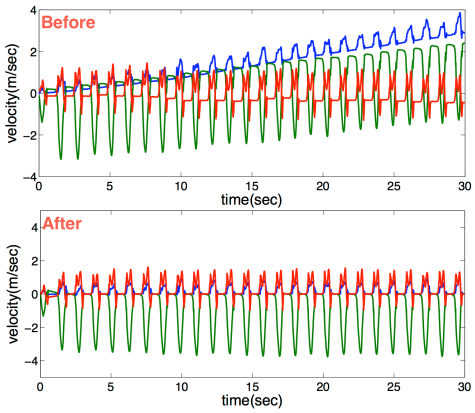

(a) ZUPT for a foot-mounted sensor

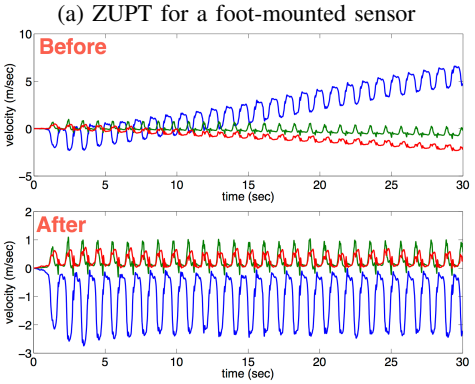

(b) non-ZUPT for ankle-mounted sensor

Fig. 5: Velocity Update Before and After Using ZUPT And Non-ZUPT Method

In addition, 4 subjects were recruited for applying the non-ZUPT algorithm to stairs walking. The training process is performed on flat floor as well and is consistent with the above. In the testing process, however, the subjects were asked to walk on stairs.

Total walking distance estimations (l^{est}) from both the ZUPT and non-ZUPT trajectory reconstruction algorithms were compared to the ground truth (l^{gt}) collected during the experiments. Estimation errors were calculated in Equation 9 and reported in Table I.

$$err = \frac{|l^{est} - l^{gt}|}{l^{gt}} \tag{9}$$

B. Results and Analysis

Figure 5 shows the velocity estimation before and after drift correction under the ZUPT algorithm and non-ZUPT algorithm. Note that only a short interval within a long walking was shown in the figure for clear visualization. Before any velocity correction algorithm, integrating the accelerations produces drifted velocity signals. The ZUPT algorithm detects stance-phases in each gait cycle and resets velocity there to be zero (Figure 5a). For the new non-ZUPT algorithm, however, we would reset the velocity at each stance-phase to an estimated value based on the estimated sensor position and gyroscope signals (Figure 5b).

Subject number	Ankle sensor (ZUPT)	Ankle sensor (non-ZUPT)	Foot sensor (ZUPT)
1	30.41%	3.63%	2.88%
2	4.24%	3.53%	0.32%
3	17.71%	6.04%	0.84%
4	16.89%	1.70%	4.00%
5	5.17%	5.44%	2.57%
6	9.17%	5.43%	0.37%
7	11.53%	4.76%	1.83%
8	16.01%	1.24%	2.54%
9	9.71%	2.22%	4.61%
10	13.55%	1.32%	3.36%
Avg.	**13.44%**	**3.58%**	**2.33%**

TABLE I: Motion Tracking Error for Flat Floor Walking

	Subject number	Ankle sensor (ZUPT)	Ankle sensor (non-ZUPT)	Foot sensor (ZUPT)
Upstairs	1	25.57%	7.00%	8.29%
	2	31.04%	1.75%	3.34%
	3	23.18%	2.44%	8.07%
	4	18.81%	3.23%	2.94%
	Avg.	**24.65%**	**3.61%**	**5.66%**
Downstairs	1	4.60%	1.06%	4.44%
	2	4.50%	4.53%	4.32%
	3	2.96%	2.80%	14.14%
	4	20.51%	7.83%	14.82%
	Avg.	**8.14%**	**4.06%**	**9.43%**

TABLE II: Motion Tracking Error For Stairs Walking

Table I shows the distance reconstruction error for different algorithms over ten subjects. Not surprisingly, the traditional ZUPT algorithm gives satisfactory trajectory estimation with 2.33% error. On the other hand, applying the ZUPT algorithm on the ankle-mounted sensor (Table I column 1) produces poor results with 13.22% error. Note that applying ZUPT to ankle-mounted sensors always underestimates the total walking distance. This is because at each stance-phase, the sensor on the ankle has positive velocity along the walking direction. Forcing them to zero with the ZUPT algorithm makes the velocity smaller than the actual values. Integrating the under-estimated velocity signals will have a cumulative effect on the distance estimation results. This systematic error can be corrected by the newly proposed non-ZUPT algorithm. The non-ZUPT algorithm estimates the actual velocity value at each stance-phase, making the trajectory estimation more accurate. Table I column 2 shows that distance estimation error was reduced to 3.58%.

Table II shows the distance estimation error for walking upstairs and downstairs. For upstairs walking, distance estimation error was reduced to 3.61% using the non-ZUPT method from 24.65% using the ZUPT method. In addition, ZUPT method is always over-estimating the walking distance. This is because, the ankle has a negative velocity at the stance-phase when walking upstairs. Forcing them to zero over-estimates the velocity, hence, over-estimates the walking distance. For downstairs walking, non-ZUPT reduces estimation error significantly only for subject No.4. For 3 other subjects, because there exists a short zero-velocity interval for each stance-phase even for the ankle-mounted sensor, performance of the ZUPT method is also acceptable. Overall, the non-ZUPT method, without the zero-velocity interval assumption is more robust over different walking styles.

IV. CONCLUSIONS

In this paper, a new non-ZUPT method was developed. This method makes single-sensor lower-body motion tracking possible for the medically more preferable ankle-mounted sensors. We use the fact that during the stance-phase, the ankle-mounted sensor is rotating around the heel. Thus, the velocity of the ankle-mounted sensor in this period can be estimated using angular velocity and the estimated rotation moment arm. The rotation moment arm is acquired through a training process with a short walking period. With this easily available training activity, we avoid the need of measuring the sensor position manually each time the sensor is mounted. Resetting velocity at the stance-phase to the estimated velocity compensates the cumulative error and estimates the final trajectory correctly.

With this method, ankle-mounted distance estimation error was reduced to 3.58% on average, compared to 13.22% on average using the conventional ZUPT method for flat floor walking. For upstairs walking, estimation error was reduced to 3.61% from 24.65%, while for downstairs walking, estimation error was reduced to 4.06% from 8.14%.

Future studies are planned to apply similar method to unhealthy gaits of neurological disease patients (e.g. stroke and Parkinson's disease). Instability, asymmetry and large variations all make this task more challenging. To solve these problems, new detection methods as well as new biomechanical models might be needed.

REFERENCES

[1] B. Dobkin and A. Dorsch, "The promise of mhealth: daily activity monitoring and outcome assessments by wearable sensors," *Neurorehabil Neural Repair*, vol. 25, no. 9, pp. 788–98, 2011.

[2] S. Patel, B. rong Chen, T. Buckley, R. Rednic, D. McClure, D. Tarsy, L. Shih, J. Dy, M. Welsh, and P. Bonato, "Home monitoring of patients with parkinson's disease via wearable technology and a web-based application," in *Engineering in Medicine and Biology Society (EMBC), 2010 Annual International Conference of the IEEE*, Aug 2010, pp. 4411–4414.

[3] Y. Wang, C. Chien, J. Xu, G. Pottie, and W. Kaiser, "Gait analysis using 3d motion reconstruction with an activity-specific tracking protocol," in *Acoustics, Speech and Signal Processing (ICASSP), 2013 IEEE International Conference on*, May 2013, pp. 1041–1045.

[4] S. Bamberg, A. Benbasat, D. Scarborough, D. Krebs, and J. Paradiso, "Gait analysis using a shoe-integrated wireless sensor system," *Information Technology in Biomedicine, IEEE Transactions on*, vol. 12, no. 4, pp. 413–423, July 2008.

[5] A. Sabatini, C. Martelloni, S. Scapellato, and F. Cavallo, "Assessment of walking features from foot inertial sensing," *Biomedical Engineering, IEEE Transactions on*, vol. 52, no. 3, pp. 486–494, March 2005.

[6] Y. Wang, J. Xu, X. Xu, X. Wu, G. Pottie, and W. Kasier, "Inertial sensor based motion trajectory visualization and quantitative quality assessment of hemiparetic gait," in *Proceedings of the 8th International Conference on Body Area Networks*, ser. BodyNets '13, 2013, pp. 169–172.

[7] B. Dobkin, X. Xu, M. Batalin, S. Thomas, and W. Kaiser, "Reliability and validity of bilateral ankle accelerometer algorithms for activity recognition and walking speed after stroke," *Neurorehabil Neural Repair*, vol. 42, no. 8, pp. 2246–50, 2011.

[8] X. Xu, M. A. Batalin, W. J. Kaiser, and B. Dobkin, "Robust hierarchical system for classification of complex human mobility characteristics in the presence of neurological disorders," in *Body Sensor Networks (BSN), 2011 International Conference on*, May 2011, pp. 65–70.